Dimerization of Xanthene Dyes in Water: Experimental Studies and Molecular Dynamic Simulations

S. Daré-Doyen,[†] D. Doizi,[‡] Ph. Guilbaud,[§] F. Djedaïni-Pilard,[||] B. Perly,[⊥] and Ph. Millié*[,#]

Institut de Radioprotection et de Sureté Nucléaire, DSMR/SACI, Bât 79, BP17, 92262 Fontenay aux Roses Cedex, Commissariat à l'Energie Atomique, DEN/DPC/SECR/LSRM, Bât 391, 91191 Gif-sur-Yvette Cedex, France, Commissariat à l'Energie Atomique, DEN/DRCP/SCPS/LCAM, Bât 166, Marcoule Cedex, France, Laboratoire des Glucides, Université de Picardie Jules Verne, 80039 Amiens Cedex, France, Commissariat à l'Energie Atomique, DSM/DRECAM/SCM, Bât 137, 91191 Gif-sur-Yvette Cedex, France, and University Paris-Sud, Bât 350, 91405 Orsay Cedex, France

Received: April 1, 2003; In Final Form: September 19, 2003

1-D and 2-D NMR experiments and molecular dynamics simulations have been performed to study the dimerization process of two laser dyes namely Rodamine 6G and Pyronine 6G in water. Two possible stacked dimer structures have been evidenced, and the agreement between experimental and theoretical results is very good. The role of dispersive and electrostatic forces in the dimerization mechanism is discussed. This analysis allows us to suggest some chemical modifications on xanthene dyes to prevent such dimerization. On this basis, a new synthesized rhodamine is described which does not exhibit any dimerization phenomenon in a large range of concentrations.

I. Introduction

Xanthene molecules are very efficient laser dyes[1−3] and fluorescent probes[4,5] thanks to their outstanding photophysical properties. They are generally used dissolved in ethanol, at a concentration lower than 10^{-2} M (mol dm^{-3}), where they exhibit a fluorescence quantum yield very close to 1. For biological applications such as high speed screening or industrial applications such as the uranium enrichment process known as AVLIS (atomic vapor laser isotope separation), it would be very convenient to operate these dyes in water. Unfortunately, in the same range of concentrations in water, the fluorescence quantum yield drops to nearly zero[6] as the result of an aggregation mechanism which is discernible at concentrations around 10^{-6} M.

Because the xanthene dyes are generally positively charged, the interaction between the two dyes is expected to be strongly repulsive. These experimental observations are therefore quite surprising: aggregation generally occurs for nonpolar neutral molecules such as alkanes in aqueous media as a consequence of the so-called hydrophobic interactions, which are also responsible for the folding up of proteins in order to "hide" their hydrophobic parts.[7] On the other hand, recent molecular dynamics simulations on aqueous solutions of picrate anions (2,4,6-trinitrophenoxide) have evidenced strong aggregate formation up to tetramers.[8] Moreover, this article clearly demonstrated that this phenomenon specifically occurs in water but not, for example, in acetonitrile. Unfortunately, these theoretical results are not yet corroborated with experimental work.

From a theoretical point of view, it seems interesting to test if numerical simulations are able to reproduce, almost qualitatively, such experimental results. From a more general point of view, the determination of all of the components of the effective hydrophobic forces leads to the finest description, at the molecular level, of these forces. From a more practical point of view, the final objective of this work being the synthesis of new water soluble laser dyes, a clear understanding of this aggregation process can help us to define some chemical modifications of these xanthene dyes in order to prevent their aggregation in aqueous solutions.

Because the limit of solubility of xanthene dyes is generally lower than 5×10^{-3} M in water and dimers are the major aggregates in 10^{-6} to $1-2 \times 10^{-3}$ M aqueous solutions, we decided, in this paper, to study the dimerization process only.

Two approaches were developed: an experimental approach using nuclear magnetic resonance (NMR) techniques to determine the dimer structure(s) and the aggregation constant(s) and a theoretical approach performing molecular dynamics simulations using the AMBER 5.0 package.[9]

^{1}H NMR was chosen among the other experimental techniques such as absorption spectroscopy or the most recent photothermal spectrometry[10] because it gives more precise information about the molecular structure and enables the determination of the dimerization constant at the same time. More precisely, a good estimation of some interatomic distances is possible allowing one to discriminate between different possible dimer structures. This is not the case for absorption spectroscopy which only gives a general idea of the dimer structure thanks to the exciton theory.[11] In the case of xanthene dyes, a blue-shifted absorption peak clearly indicates that the two molecules lie in parallel planes (H aggregate). However, first, it is not possible to distinguish between parallel and antiparallel structures. Besides, no quantitative description of the dimer geometry can be obtained because the Förster formula,

* To whom correspondence should be addressed.
[†] Institut de Radioprotection et de Sureté Nucléaire.
[‡] Commissariat à l'Energie Atomique, DEN/DPC/SECR/LSRM.
[§] Commissariat à l'Energie Atomique, DEN/DRCP/SCPS/LCAM.
[||] Université de Picardie Jules Verne.
[⊥] Commissariat à l'Energie Atomique, DSM/DRECAM/SCM.
[#] University Paris-Sud.

10.1021/jp034845j CCC: $25.00
Published on Web 11/20/2003

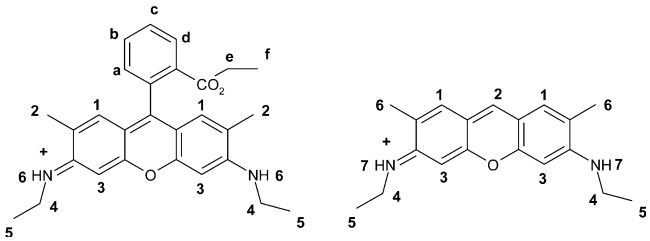

Figure 1. Rhodamine 6G and Pyronine 6G.

using the dipolar interaction between transition moments, cannot be applied in such situations.[12]

Molecular dynamics simulations were performed with the different following purposes: first, to compare the theoretical dimer structure(s) to the experimental one(s), which is an excellent test to probe the capacity of molecular dynamics simulations to predict dimerization for similar systems; second, to understand the respective role of the interaction between dyes and the interactions of dyes with water molecules and counterions in the dimerization phenomenon; finally, of course, to determine, on the basis of these results, the different ways to prevent the dimerization process.

The dyes which were studied are Rhodamine 6G and its pyronine analogue, Pyronine 6G, shown in Figure 1. They were respectively chosen, the first one for its very frequent use as a laser dye and the second one as a simpler model of such dyes. Both of them contain the same chromophoric part, three flat conjugated cycles called chromophores which are responsible for the photophysical properties. The Rhodamine 6G carbethoxyphenyl group is nearly perpendicular to the chromophore and is therefore responsible for some steric constraints. Thus, aggregation properties are expected to be of minor importance for Rhodamine 6G compared with Pyronine 6G.

II. Methods

II.a. Experimental Methods. All NMR experiments were performed at 500.13 MHz using a Bruker DRX500 spectrometer equipped with a *Z*-gradient unit for pulsed-field gradient spectroscopy. Me_4Si was used as an external standard and calibration was performed using the signal of the residual protons of the solvent as a secondary reference. Measurements were performed at 298 K with careful temperature regulation. The length of the 90° pulse was 7.0 μs. 1D NMR data spectra were collected using 16K data points. 2D experiments were run using 1K data points and 256 time increments. The phase sensitive (TTPI) sequence was used and processing resulted in a 1K × 1K (real-real) matrix.

Rhodamine 6G with chloride counterion was purchased from Kodak Inc. and was used without further purification. Pyronine 6G was synthesized in our laboratory. Samples were prepared by volumic dilution of a concentrated dye−deuterated water D_2O solution made at the limit of solubility. They were lyophilized 3−4 times before analysis. The concentration of the initial solution was determined by the measurement of the optical density of lyophilized samples dissolved in ethanol. The chosen concentration range corresponds to solutions in which *n*-mers ($n > 2$) can be neglected. In these conditions, experimental data were analyzed in terms of a simple monomer−dimer equilibrium.

In the case of Rhodamine 6G, the dimer structure was determined thanks to ^{1}H NMR and ROESY experiments (rotating frame NOE two-dimensional spectroscopy). 2D ROESY experiments were realized instead of the generally used NOE (nuclear overhauser enhancement) because NOE (which is directly dependent on molecule size) has unfortunately a non measurable value for our samples.[22]

T-ROESY (transverse ROESY) experiments with mixing times ranging from 80 to 320 ms allowed the determination of typical intermolecular distances *d*: the curves representing the correlation spot integrated volumes versus mixing times were plotted for both the studied intermolecular coupling and an intramolecular coupling (in this case, coupling between H_a and H_b, shown in Figure 1, was chosen, $d = 2.47$ Å). As the curve slope at the origin is proportional to $(1/(\text{distance})^6)$, the unknown distance can be estimated thanks to the reference given by the intramolecular coupling curve. It can be noticed that such a method cannot be applied in the pyronine case.

The dimer formation constant *K* was determined by using the value of the chemical shift δ of the chromophore protons H_1, H_2, and H_3 (shown in Figure 1) measured in spectra obtained for, at least, six different dye concentrations *C*. Only chromophore protons were used because they are fixed on a rigid structure so that the variation of their chemical shift is only a consequence of the dimer formation and not of conformational changes.

Starting from estimated δ_D, δ_M, and *K* values, a computational simulation based on the following relationships:

$$\delta_{obs} = ([M]\delta_M + 2[D]\delta_D)/C \qquad (1)$$

$$\text{with } K = [D]/[M]^2 \text{ and } C = 2[D] + [M]$$

(δ_{obs}, δ_M, and δ_D are respectively observed, monomer and dimer chemical shift) led to the optimized δ_D, δ_M, and *K* values through reiterated calculations with the least-squares method.

II.b. Simulation Methods. Molecular dynamics simulations were performed with the AMBER 5.0 package[9] using the Cornell et al. all-atom force field and with the following description of the potential energy:

$$E = \sum_{\text{bonds}} K_b[b - b_0]^2 + \sum_{\text{angles}} K_\theta[\theta - \theta_0]^2 + \sum_{\text{dihedrals}} \frac{V_n}{2}[1 + \cos(n\varphi - \delta)] + \sum_{i,j}\left[\frac{q_i q_j}{\epsilon r_{ij}} + \left(\frac{A_{ij}}{r_{ij}^{12}} - \frac{B_{ij}}{r_{ij}^{6}}\right)\right]$$

Some parameters, namely force constants and equilibrium values for some bonds, angles, and dihedrals, are not defined in the initial force field. These data mainly concern the aromatic oxygen of the xanthylium part. From a formal point of view, an aromatic nitrogen atom can take the place of this oxygen atom. We have used this analogy for the definition of these unknown parameters (all these values can be obtained upon request to the authors) in the harmonic part of the potential energy.

The partial charges are obtained from a 6-31G Hartree−Fock calculation in the equilibrium geometry using the ESP (electrostatic surface potential) procedure as implemented in the Gaussian 98 package.[13] The charges on atoms equivalent for symmetry reasons as well as the charges on chemically equivalent atoms, namely, the hydrogens of CH_3 and $-CH_2-$ chemical groups, exhibit values averaged on the previous corresponding ESP charges. These charges are shown in Figure 2. Some supplementary calculations have been performed on the Rhodamine 575 (see discussion hereafter). The corresponding charges are also shown on the same figure.

The simulations were performed in aqueous solutions using an explicit representation of the solvent. The model used for the description of water is the well-known TIP3P[14] one. The

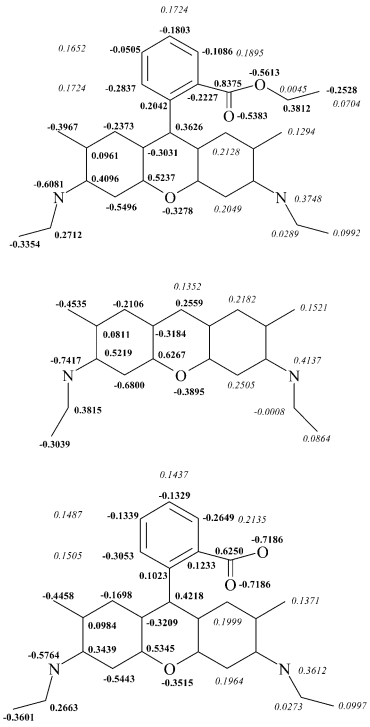

Figure 2. ESP atomic charges on Rhodamine 6G, Pyronine 6G and Rhodamine 575. **Charge** corresponds to carbon, oxygen, and nitrogen, *charge* deals with hydrogen.

TABLE 1: General Conditions of the Performed Molecular Dynamics Simulations

	no. of water molecules	conc., mM	box size after equilibration (Å × Å × Å)
Rhodamine 6G-starting with dimer1 formed	1798	62	34 × 41 × 40
Rhodamine 6G-starting with unstacked arrangement	1864	60	34 × 42 × 40
Rhodamine 575- starting with unstacked arrangement	1388	80	35 × 36 × 35
Pyronine 6G- starting with dimer1 formed	1276	87	34 × 36 × 32
Pyronine 6G- starting with dimer2 formed	1017	109	33 × 36 × 26

electroneutrality of the solution is ensured by adding a chloride anion for each positively charged dye molecule.

Solute molecules were placed in a water box with periodic boundary conditions using a 12 Å cut off.[8] All of the molecular dynamics calculations were run at constant pressure (1 atm) and at constant temperature. The temperature was maintained at 298 K with the Berendsen algorithm using separate scaling factor for atoms of the solute and atoms of the solvent.

A time of 2 fs was set for the integration step. For this purpose, the X−H stretching modes were frozen, using the SHAKE algorithm. Moreover, the long range electrostatic forces can be of great importance. So to properly take into account these interactions, the Ewald summation technique has been chosen. It was checked that these long-range forces have no great influence on the dimer structure (see below). Consequently, most of the simulations were performed without the Ewald summation.

Table 1 shows the general conditions of the performed molecular dynamics simulations. Because there are two dye molecules in each water box, the resulting concentration ranges between 6×10^{-2} and 10^{-1} M. This is 20−100 times more than the highest concentration experimentally studied. Simulating the experimental conditions was not possible due to computational limitations. Nevertheless, the comparison of the theoretical dimer structure with the experimental one is meaningful because the dimer structure obtained without interaction between dimers (no Ewald correction) and the one obtained when these interactions are taken into account by the Ewald procedure are quite similar.

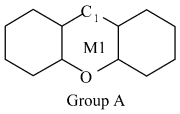

Figure 3. M is the barycenter of the 14 atoms of the xanthylium group A. P is the average plane of group A. Parameters used to define the dimers geometries: α angle = angle between P1 and P2; β torsion = $C_1-M1\cdots C_2-M2$; M−M distance = M1···M2; M−chromophore distance = average between M2···P1 and M1···P2.

The simulation procedure is the following: Two dye molecules, in their in vacuo optimized geometry, are set in the water box. Thanks to the knowledge of the electrostatic potential created by each dye molecule, the chloride counterions are initially located in an energetically favorable position. This box is then heated to 298 K. The equilibration procedure is done in two steps. The first corresponds to the relaxation of the water molecules, the position of the dye molecules and of the counterion being frozen. This equilibration is performed on a period of about 150 ps, until a density close to 1 (1 ± 0.02) was reached.

In the second step, the constraints on the dye molecules and the counterions are removed. About 15 additional ps are needed for the total achievement of the equilibration procedure.

After that, starting from the equilibrated system, MD trajectories were recorded during a maximum of 700 ps in order to characterize the dimer structures.

The dimer geometries were described by determining distances and torsions between the chromophores as shown in Figure 3. PMF (potential of mean forces) calculations were performed using the Gibbs free energy perturbation theory in order to obtain the free energy difference between the two dimer structures (parallel or antiparallel).

III. Results

III.a. Experimental Studies. The first observation is the progressive change of the 1D ^{1}H NMR spectrum with the initial concentration, which is an evidence of the dimerization process. Whatever the concentration studied, no additional peak was observed compared to the monomer spectrum. This is specific of a quick exchange between different species which leads to the observation of an unique average signal whose chemical shift depends on species quantities and their respective chemical shifts. Thus, NMR observations point out the formation of a monomer−dimer equilibrium. A complete assignment of all of the resonances has been performed by COSY, successive RELAY, HMQC, and HMBC experiments.

The dimer formation constant K for Rhodamine 6 G was determined by solving eq 1 using the chemical shift δ of the chromophore protons H_1 and H_3 measured in spectra obtained for six different concentrations. The dimer formation constant K for Pyronine 6G was determined, in the same way, by measuring the chemical shift δ of the chromophore protons H_1, H_2, and H_3 in spectra obtained for seven different concentrations.

The experimental results are summarized in Table 2.

The association constant K was calculated to be 1000 for Rhodamine 6G and 4000 for Pyronine 6G at 298 K. This value is obtained by averaging the K values calculated for each

TABLE 2: Chemical Shift (ppm) of the Rhodamine 6G and Pyronine 6G Chromophore Protons versus Concentration (Top) and Changes in Chemical Shift between the Dimer and the Monomer (Bottom) and Association Constant in D_2O at 298 K

Rhodamine 6G			Pyronine 6G			
conc., mM	δH_1	δH_3	conc., mM	δH_1	δH_2	δH_3
3.43	6.909	6.451	1.35	6.918	7.603	6.200
1.71	6.924	6.542	1.01	6.972	7.669	6.255
0.86	6.941	6.625	0.68	7.042	7.749	6.320
0.43	6.956	6.698	0.51	7.099	7.817	6.376
0.21	6.972	6.769	0.34	7.180	7.915	6.458
0.086	6.998	6.869	0.17	7.344	8.118	6.622
			0.084	7.502	8.319	6.783

$\Delta\delta_H = \delta_M - \delta_D$	Rhodamine 6G	Pyronine 6G
$\Delta\delta_{H1}$	0.15 = 7.01−6.86	1.35 = 7.90−6.55
$\Delta\delta_{H3}$	0.73 = 6.96−6.23	1.37 = 7.22−5.85
$\Delta\delta_{H2}$	1.70 = 8.88−7.18	
K (M^{-1})	1000 ± 300	4000 ± 500

chromophore protons H_1, H_2, and H_3. It is not possible to determine K with a great accuracy because of concentration range limitations: the concentration should be higher than 8×10^{-5} M because of NMR detection limits and smaller than 4×10^{-3} M because of dyes solubility limit.

The value, $K = 1000\ M^{-1}$, calculated for Rhodamine 6G is lower than the one published in the literature using the absorption spectroscopy method; some authors have measured K to be 1700,[1] 1690,[2] 1500,[15] or 2580 [16] at 295 K and 1800 at 279 K.[5] The discrepancies between these data may be explained by the large approximations on the value of the dimer extinction coefficient or the deviations on cell length, especially for small cells whose length is around 100 μm and which are used to study 10^{-3} M solutions. With the same technique (absorption spectroscopy), Sens and Drexhage[17] measured K to be 3300 and 12 000 for Rhodamine 6G and Pyronine 6G, respectively, showing a similar ratio between the two association constants (1−3.6 instead 1−4). These results may be interpreted as the consequence of the steric hindrance of the carbethoxyphenyl group which interferes in the dimer formation. Concerning Pyronine 6G dimerization constant, no other reference was found in the literature.

The dimer structures were determined as follows: The analysis of proton spectra with increasing concentrations, i.e., with dimer proportion raising in solution, shows important chemical shift variations for some protons as shown in Table 2. For Rhodamine 6G, $\Delta\delta_H$ is larger for H_3 than for H_1. Consequently, protons H_3 of a dye molecule are expected to undergo an aromatic anisotropy because of the chromophore aromatic cycle and the carbethoxyphenyl group of the other dye molecule. The dimer structure looks like stairs, that is to say that the two chromophores in the dimer are "shifted" (parallel displaced structure). On the other hand, T- ROESY contour plots show a strong interaction between proton H_a and H_3 as shown in Figure 4.

The intramolecular experimental distance H_a-H_3 is greater than 4 Å which leads us to the conclusion that this H_a-H_3 dipolar interaction is an intermolecular one. This is exactly the same conclusion for the interactions between H_1 and *N*-ethyl protons or for H_3 and methyl group protons. As a result, we can conclude that the two chromophores are antiparallel, one over the other, and that, due to the presence of the H_a-H_3 interaction and the lack of an interaction between the ethoxy protons and H_3, the carbethoxyphenyl groups are trans outward positioned as described in Figure 5. The $(1/H_a-H_3 \text{ distance})^6$ is (1/2.68 Å).[6] This structure is consistent with the previous NMR studies[4] in which the dimers exhibit a stacked structure of the xanthene rings with the benzoate rings oriented outward but differs from the dimer model suggested by optical absorption data. In these papers, dimers are also constituted of two antiparallel stacked entities, but the carbethoxy group are oriented inward[18] or cis.[19] Differently, $\Delta\delta_H$ is the same for H_3 and H_1 in Pyronine 6G which leads us to the conclusion that, in this case, the two chromophores are strictly face to face. The two chromophores are antiparallel which is probed by weak interactions between H_3 and H_1, H_3 and the methyl group, and H_1 and *N*-ethyl protons.

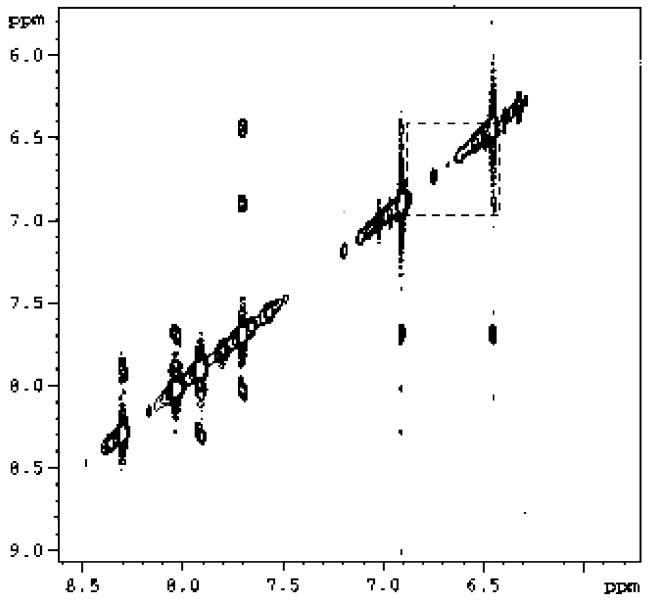

Figure 4. Contour plot of T-ROESY experiment (300 ms of spin lock, 22dB attenuation) performed on Rhodamine 6G (3.43 mM, 298 K, D_2O, 500.13 MHz).

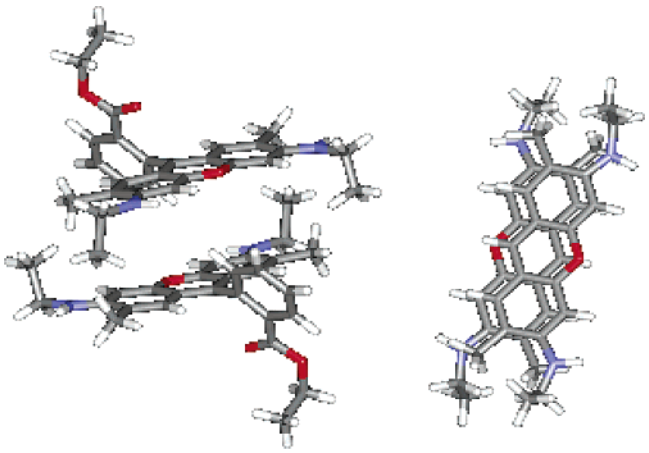

Figure 5. Representation of a possible dimer structure determined by NMR analysis for Rhodamine 6G and Pyronine 6G.

III.b. Molecular Dynamics Simulation Results. We have first performed molecular dynamics simulations with the two dye molecules in the water box lying initially in parallel planes, in a configuration corresponding to the NMR experimental results. To prevent us from any possible artifact and to really prove the dimer formation phenomenon, we have also performed simulations starting from two separated dye molecules.

1. Initially Created Dimer. Starting with the dimer structure deduced from NMR results analysis (this structure is called dimer 1 in the following), we have performed molecular

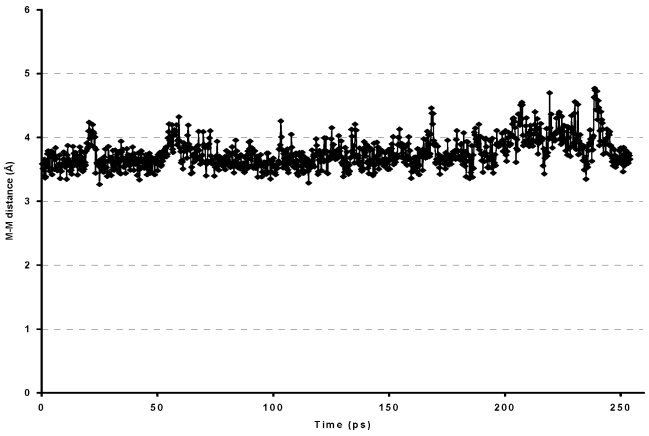

Figure 6. M−M distance in the Rhodamine 6G dimer 1 during the simulation.

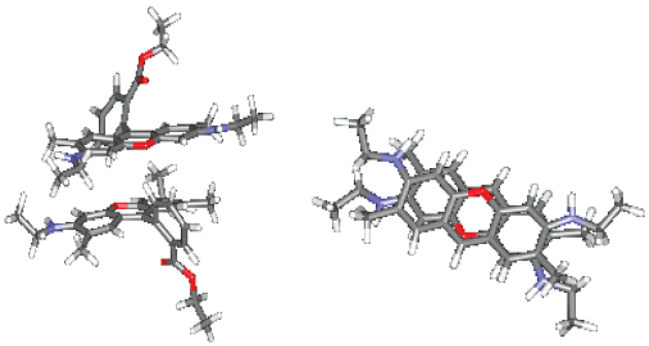

Figure 7. Snapshots of dimers determined by MD simulations for Rhodamine 6G (left) and Pyronine 6G.

dynamics simulations using the procedure previously described, for both Rhodamine 6G and Pyronine 6G dimer.

For both dyes, we observed a total stability of the dimer during all of the simulated time, i.e., 700 ps as shown in Figure 6 for the first 250 ps.

Clearly, the M−M distance oscillates around a mean value of 3.8 Å in the Rhodamine 6G dimer. Thus, on the average, the dimer can be described by two nearly antiparallel stacked entities (α angle is 10°), one chromophore on the top of the other separated by an average plane-plane distance of 3.5 Å for Rhodamine 6G and 3.4 Å for Pyronine 6G. For Rhodamine 6G, it must be pointed out that the two carbethoxyphenyl groups are trans outward positioned. Moreover, the chromophores are not strictly face to face as shown in Figure 7. Conversely, in the Pyronine 6G case, the two chromophores exhibit a perfectly stacked mean structure (Figure 7).

The average distance between the two planes is in the same range of values as the usually reported ones: for example in picrate dimers,[8] the M−M distance is calculated to be about 3.7 Å corresponding to a plane-plane distance of 3.5 Å. Moreover, we obtain an H_a-H_3 distance equal to 2.74 Å, very close to the experimental one (2.68 Å). This fact leads us to have some confidence in our MD simulation results.

The evolution of the different data during MD reveals that the 2 molecules in the dimer have a libration movement around an axis perpendicular to chromophores, which is responsible for the oscillation of the torsion angle β. However, this motion is larger for Pyronine 6G than for Rhodamine 6G as shown in Table 2. At the same time, Pyronine 6G molecules are subject to important "jiggling" in dimers as it is probed by the M−M distance which is greater for Pyronine than for Rhodamine.

At least, it must be noticed that the Ewald correction does not significantly alter the previous results. For example, the H_a-H_3 distance increases by only 0.02 Å (2.76 versus 2.74 Å). In the same way, the mean distance between the two chromophore planes decreases by only 0.04 Å (from 3.51 to 3.47 Å; see also Table 3).

TABLE 3: Averaged Geometrical Parameters without Ewald Correction[a]

	Rhodamine 6G		Pyronine 6G	
	dimer 1	dimer 2	dimer 1	dimer 2
M−M distance (Å)	3.80 ± 0.22 *3.75 ± 0.23*	4.28 ± 0.29 *4.59 ± 0.39*	4.14 ± 0.52	4.03 ± 0.43
plane−plane distance (Å)	3.51 ± 0.16 *3.47 ± 0.32*	3.65 ± 0.18 *3.65 ± 0.17*	3.43 ± 0.25	3.48 ± 0.18
$1/(\text{distance } H_a-H_3)^6$ $(1/\text{Å})^6$	2.74 *2.76*			
α angle (deg)	5 ± 3 *10 ± 6*	12 ± 5 *13 ± 5*	9 ± 8	8 ± 6
β torsion (deg)	10 ± 11 *20 ± 11*	174 ± 13 *165 ± 11*	4 ± 18	177 ± 17

[a] Italic parameters for Rhodamine 6G (second line) derived from calculations using Ewald correction.

2. Initially Separated Dyes. A second series of simulations was performed for both dyes, starting with separated monomers, i.e., with a M−M distance greater than 10Å. For rhodamine 6G, starting from equilibrated configurations such as the one described in Figure 8, the formation of a dimer occurs before 240 ps.

Using different initial conditions, two structures may be obtained: The first one is the antiparallel stacked dimer 1 already described before, which is in agreement with the NMR analysis. This last result is an unambiguous evidence of the existence of this dimer. The second one, dimer 2, can be described as two parallel stacked entities (Figure 8). The distance between the two planes is a little larger in this dimer (3.65 instead of 3.51 Å).

Because of the steric repulsion between the two carbethoxyphenyl groups, the chromophores are quite shifted as proved by the great difference between the M−M distance and plane−plane distance. At the same time, the two carbethoxyphenyl groups are trans positioned, and we can observe the same motion as the one observed in dimer 1 which is responsible for the oscillation of the β torsion.

This structure exhibits a stability quite similar to the one observed in dimer 1. No separation or conversion process into dimer 1 is observed during the molecular dynamics simulations. The same simulations, but performed at higher temperatures (400 K), lead to the same results (no conversion of dimer 1 into dimer 2). So a non-negligible activation barrier prevents any fast conversion between the antiparallel (dimer 1) and parallel (dimer 2) entities.

Starting from different configurations before equilibration, we tried to observe the same phenomena for pyronine 6G. However, unfortunately, either the dimer formation was never observed or, in the other cases, the dimer was already formed at the end of the second equilibration (when solute atoms are free). In this case, the stability of the corresponding dimer 2 was tested over 600 ps and no dimer breaking up was observed.

So we can conclude that, at least in the theoretical calculations, the dimer can exist under two different forms for the two molecules studied.

IV. Discussion

Two key points have to be discussed at this stage. The first one is connected with the ultimate goal of this study, namely,

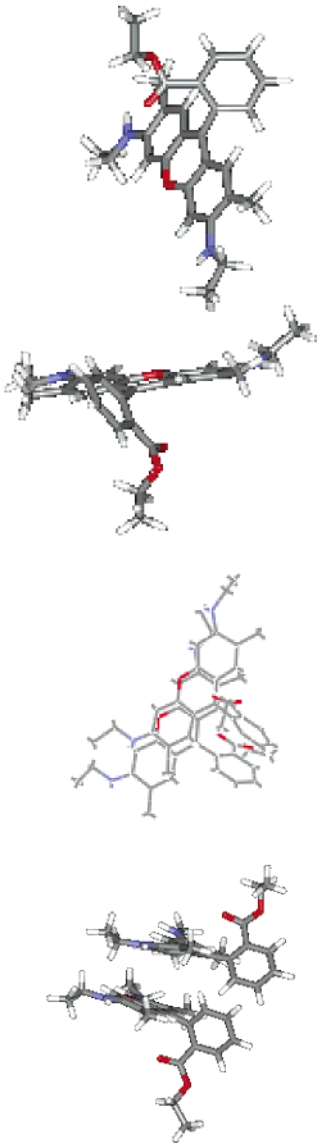

Figure 8. Starting configuration (M−M distance = 10.30 Å) and dimer 2 structure.

the design of xanthene derivatives in order to prevent the dimerization process in aqueous solutions. For this purpose, a relation between the calculated dye−dye interaction in dimers and experimental equilibrium constant would be very useful. The second point concerns the exactness of the theoretical prediction concerning the existence of two possible configurations for the dimer. Indeed, the interpretation of results obtained in NMR or photoabsorption experiments is closely related to the answer to this last question.

IV.a. Dimerization Mechanism. 1. Dye−Dye Interaction. The dye-dye interactions for the two studied molecules and the two dimers are shown in Table 4.

As expected, the electrostatic energy component of this interaction is repulsive in all cases. As also expected, the van der Waals interaction, which is attractive in all cases, is greater in Rhodamine 6G dimers than in Pyronine 6G one and no appreciable difference in the total dye-dye interaction energy occurs between dimer 1 and dimer 2. The total interaction energy is strongly repulsive in the four cases. However, the most puzzling result is that this repulsive interaction is definitely greater in the pyronine case, whereas the corresponding equilibrium constant is greater than the Rhodamine 6G one (almost

TABLE 4: Energy Components Analysis

	Rhodamine 6G		Pyronine 6G	
	dimer 1	dimer 2	dimer1	dimer 2
E dye−dye (kcal/mol)				
$E_{\_tot}$	21.4 ± 1.4	22.7 ±1.4	29.1 ± 1.4	29.3 ± 1.4
$E_{\_el}$	42.8 ± 1.1	43.2 ± 1.3	45.8 ± 1.4	46.5 ± 1.5
$E_{\_VdW}$	−21.4 ± 1.5	−20.5 ± 1.5	−16.7 ± 1.3	−17.2 ± 1.3

TABLE 5: Mean Geometrical Characteristics and Dye−Dye Interaction Energies (in kcal/mol) for Rhodamine 6G and Rhodamine 575 Antiparallel Dimers (Data Obtained with Ewald Summation Technique)

	Rhodamine 6G dimer	Rhodamine 575 dimer
Geometrical Parameters		
M−M distance (Å)	3.75 ± 0.23	3.90 ± 0.29
plane−plane distance (Å)	3.47 ± 0.32	3.53 ± 0.17
α angle (deg)	10 ± 6	8 ± 5
β torsion (deg)	20 ± 11	20 ± 16
Dye−Dye Interaction Energy		
total energy	21.4 ± 1.4	−20.4 ± 1.8
electrostatic energy	42.8 ± 1.1	1.1 ± 0.8
van der Waals energy	−21.4 ± 1.5	−21.5 ± 1.5

a factor of 3.6 in ref 17). It will be also noticed that the plane−plane distance is a little shorter in pyronine dimers.

So, we decided to theoretically study the dimer of Rhodamine 575 which is a zwitterion of zero global charge. The reasons for this choice are the following. First, it is expected that the electrostatic interaction is not as strong as in Rhodamine 6G dimers, the dispersion energy component being, on the contrary, almost the same. Second, the experimental equilibrium constant is close to the Rhodamine 6G one (K575/K 6G = 0.72). The same general simulation protocol was applied, the only difference being the lack of any counterion.

These simulations lead to the same observations as for Rhodamine 6G. The formation of a parallel and an antiparallel dimer is evidenced. Both dimer structures are very similar to the structures described above for Rhodamine 6G.

As depicted in Table 5, the average plane−plane distance in antiparallel structure is 3.53 Å which is close to those observed for Rhodamine 6G, 3.47 Å. On the other hand, the mean dye−dye interaction energy which is repulsive in the case of Rhodamine 6G is attractive for Rhodamine 575 (−20.4 kcal/mol). The van der Waals component, −21.5 kcal/mol, is identical to the one observed for Rhodamine (−21.4 kcal/mol), but the electrostatic interaction is very weakly repulsive, 1.1 kcal/mol instead of 42.8 kcal/mol in the Rhodamine 6G case.

These results are not in agreement with the experimental equilibrium dimerization constants of these dimers which are almost the same! The chemical design of nondimerized dye molecules in aqueous solutions cannot be build only on this dye−dye interaction. In fact, the suitable way for this purpose is very probably the use of the hydrophile and hydrophobe effective forces concept.[7] From this point of view, the dimerization of rhodamine derivatives is a very interesting case: on one hand, it is well-known that the $(NRR')^+$ chemical group is an hydrophilic group. On the other hand, the attractive hydrophobe effective forces exhibit a significant extent between two aromatic molecules. Clearly, the second effect is greater than the first one, leading to the dimerization phenomenon. It can be also noticed that the structures experimentally and theoretically observed always correspond to a "contact" structure: no water molecule lies between the two chomophoric planes.

2. Dimerization Process. When molecular dynamic simulations are performed with initially separated dyes, one can

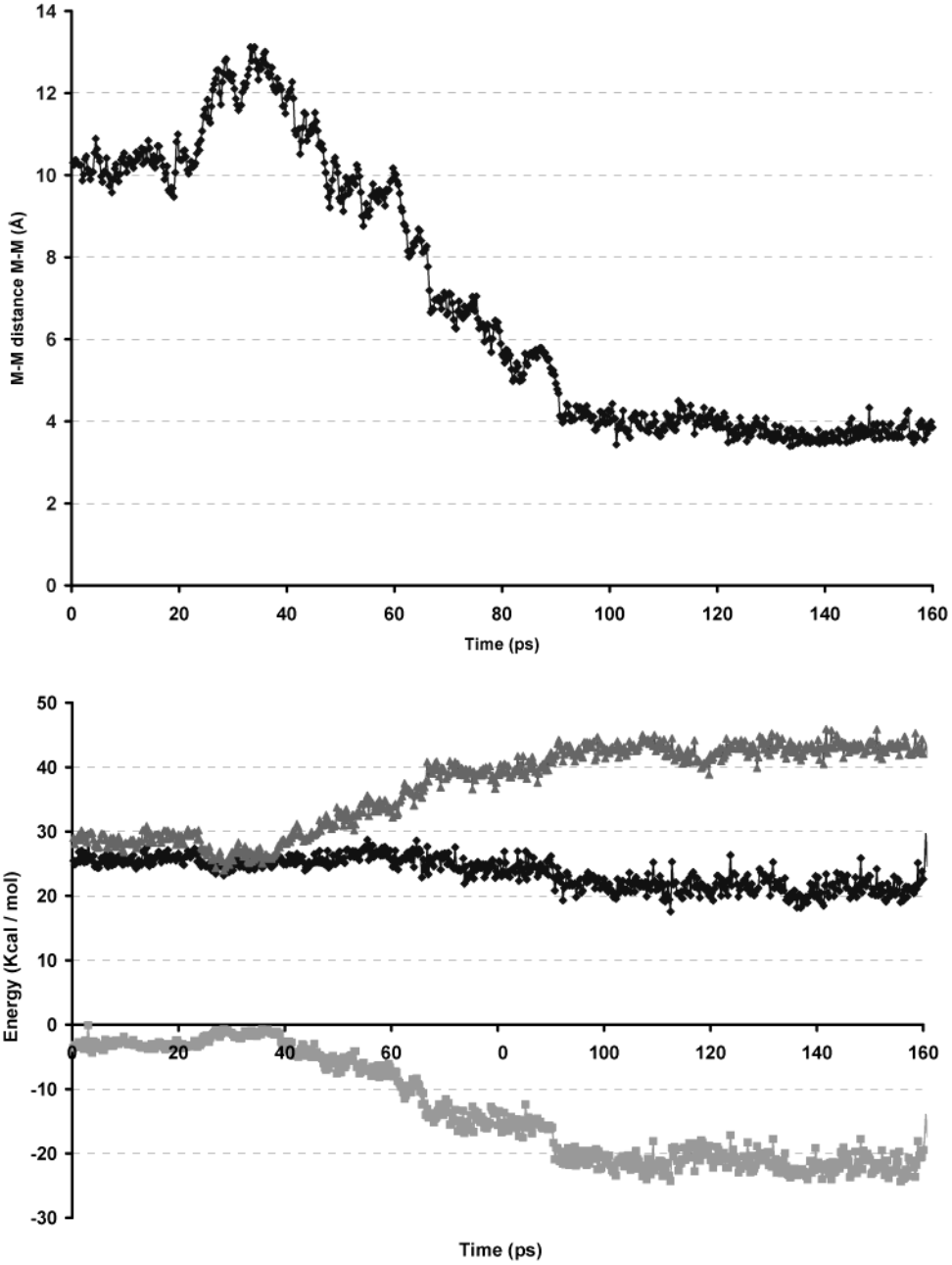

Figure 9. van der Waals component of the dye−dye interaction (lower plot), electrostatic component (upper plot) and the sum of the two interactions (middle plot).

observe the variation of the various components of the total potential energy during this dimerization process. Two interactions are particularly interesting: the interaction between dyes on one hand and the interaction of each dye with the solvent and the counterions on the other hand.

Figures 9 and 10 show the variations of these energies and their components during simulated formation of the Rhodamine 6G dimer.

(i) Dye−Dye Interaction. Figure 9 shows the van der Waals component of the dye−dye interaction (lower plot), the electrostatic one (upper plot), and the sum of these two interactions (middle plot). Clearly, the van der Waals attractive interaction increases continuously from almost 0 to about 20 kcal/mol.

On the other hand, the repulsive electrostatic energy increases, but more slowly. Consequently, the total dye−dye interaction is less repulsive in the dimer than in the separated dyes system (by about 5 kcal/mol). A possible explanation lies in the fact that, at a short intermolecular distance, the electrostatic interaction is clearly smaller than $1/R$ (by a factor greater than two at the equilibrium geometry of the dimer), due to the large delocalization of the charge on the Rhodamines.

(ii) Rhodamine−(Water and Counterions) Interaction. Figure 10 shows the variation of the electrostatic and van der Waals components of Rhodamine−(water and counterions) interaction. As expected, the van der Waals component is less attractive when the dimer is built than in the separated species. However, the electrostatic interaction between the two Rhodamines and their environment (counterions and water molecules) favors the dimerization. The total interaction increases by about 30 kcal/mol. So, the dye−dye interaction as well as the interaction of the two dyes molecules with their environment favor the dimerization process.

IV.b. One or Two Dimers? 1. Experimental Evidence of the Coexistence of Parallel and Antiparallel Pyronine Dimer

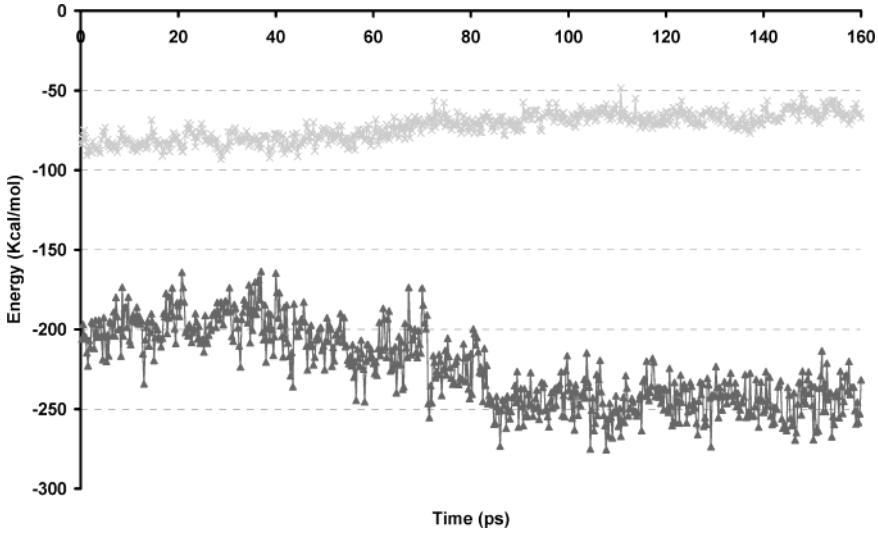

Figure 10. Electrostatic (lower plot) and van der Waals (upper plot) components of Rhodamine−(water and counterions) interaction.

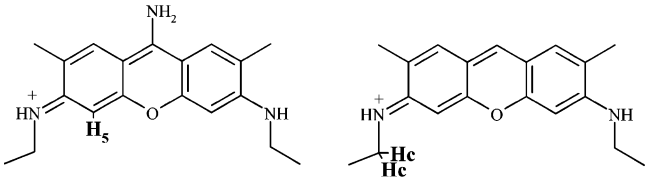

Figure 11. Pyronine *12*[20] and pyronine 6G.

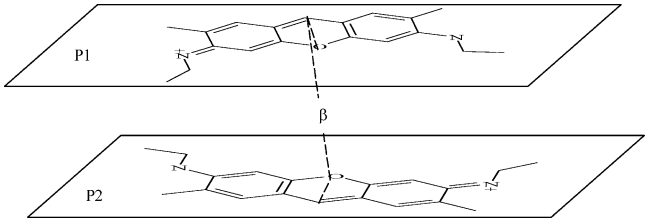

Figure 12. Definition of the dihedral angle β.

in Aqueous Solutions. Molecular dynamics simulations suggest the existence of two types of dimer structures, whereas only one of them was observed by NMR analysis on samples containing one molecule type. These results raise the question of parallel structures, especially because these species are not detectable by NMR experiments: it is impossible to identify specific intermolecular interactions because of the dimer symmetry.

To answer this question, some complementary experimental studies were realized with Pyronin 6G. T-ROESY experiments were performed with a sample containing $^1/_4$ Pyronin *12*[20] and $^3/_4$ Pyronine 6G (Figure 11) in deuterated water, at 298 K, with a maximum concentration of heterodimer around 0.34 mM. The spectrum shows a dipolar interaction between proton H_5 and proton H_c. Such an interaction can only be observed if one molecule is on the top of the other in a parallel configuration. So these results clearly prove the presence of parallel heterodimer.

This evidence of parallel structure for heterodimers suggests the existence of this kind of dimer for two identical dyes.

2. Theoretical Interpretation of NMR Results. As discussed above, NMR experiments have evidenced the coexistence in aqueous solutions of two dimers in the pyronine case. This implies that there is no interconversion between the two forms, at NMR time scale, and that the two local minima have to be separated by an enough free energy barrier. Moreover, as the two dimers are observed, their equilibrium constants have to be approximately equal. From a theoretical point of view, a potential mean force (PMF) calculation starting from dimer 1 and leading to dimer 2 (and reverse way) allows us to answer these two questions. This calculation has been first performed for the pyronine 6G. In this case, the two dimers correspond to perfectly stacked parallel and antiparallel structures. The easiest connecting path is the slow modification of the β dihedral angle (as defined in Figure 12) from 0° to 180° and from 180° to 0°.

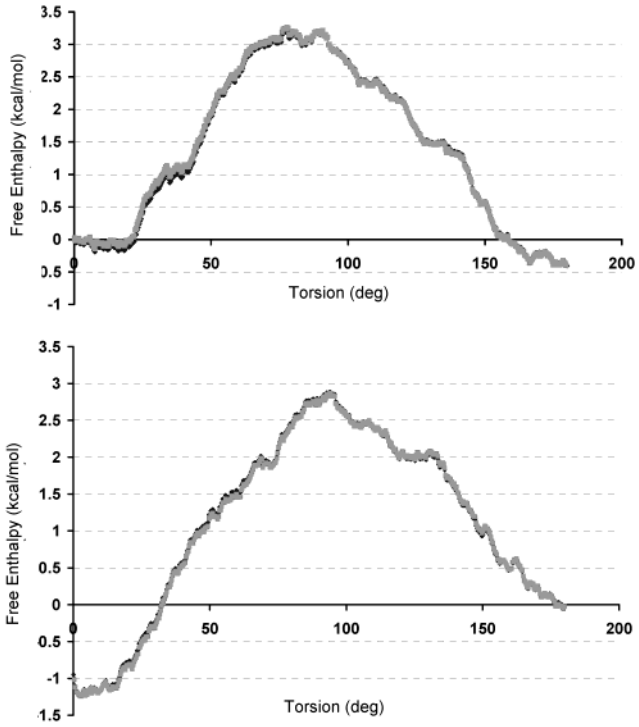

Figure 13. Free enthalpy variation. The curve on top deals with antiparallel (0°) to parallel structure (180°), whereas the one at the bottom is about parallel (180°) to antiparallel structure (0°).

For this simulation, the free energy perturbation window growth method was used.

Each "window" corresponds to an increment of $\delta\beta = 0.36°$. Five hundred windows are then necessary to transform one dimer in the other. This increment can appear as very small. However, as the Pyronine 6G exhibits a big size, a torsion of 0.36° corresponds to a non-negligible movement of the most remote atoms which lie at almost 8 Å of the rotation axis.

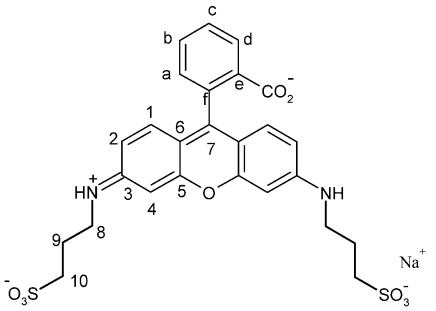

Figure 14. New Rhodamine dye synthesized in our laboratory.

At each step, an equilibration calculation of 2 ps is followed by a molecular dynamics calculation of 2 ps to collect the needed data. The variation of the free enthalpy along the path 0° → 180° is shown in Figure 13 (top). The reverse path 180° → 0° is shown on the bottom of the same figure.

The hysteresis phenomenon is small, and we can have therefore some confidence in the reliability of our calculations. On average, the free enthalpy variation between the two dimers is almost 0, leading to equivalent dimerization equilibrium constants and consequently equivalent concentrations. This fact explains why the two dimers can be separately observed in NMR experiments.

The attractive hydrophobic effective potential between the two molecules is a minimum for $\beta = 90°$, leading to an activation energy barrier of about 3 kcal/mol. It is interesting to note that, for this angle, the interaction energy between the two dyes, which is very repulsive for $\beta = 0°$ and 180° (Table 3), is now attractive by about 5 kcal/mol, confirming that the dye−dye interaction alone cannot explain the results. This free energy barrier explains why, in previously described simulations, no conversion from a dimer to the other is observed on a nanosecond time scale.

Unfortunately, in the case of the Rhodamine 6G, an analogous PMF calculation is difficult to perform. During the torsion motion and specially around $\beta = 90°$, one carbethoxyphenyl group bangs against the other and the curve depicting the free energy evolution always increases. In these conditions, no simple path connecting the two structures can be found. Nevertheless, our NMR experiments seem to prove that, for Rhodamine 6G, the antiparallel structure is clearly more stable than the parallel one. This conclusion is corroborated by ROESY NMR experiments on samples containing Rhodamine 6G and Rhodamine B in deuterated water at 295° K:[4] no heterodimer with parallel structure was detected. An explanation of this difference between Pyronine and Rhodamine possibly lies in the fact that, because of the steric hindrance between the carbetoxyphenyl groups, the parallel dimer exhibits a structure more far from a perfect stacked one than the antiparallel dimer. Indeed, the M−M mean distance is significantly greater in the dimer 2 than in the dimer 1 (a perfect stacked structure corresponds to a reverse situation as seen for pyronine). Moreover, the plane−plane distance is also greater in dimer 2 than in dimer 1. So the hydrophobic forces are significantly greater in the antiparallel than in parallel structure, leading to a dominating occurrence of dimer 1 (antiparallel structure) in aqueous solutions of Rhodamine derivatives.

3. Dimerization Equilibrium Constant Measurements in the Pyronine Case. In the exciton theory framework, as previously discussed, absorption curves of perfectly stacked structures are identical. In this case, it is very easy to demonstrate that the equilibrium constant *K* deduced from photoabsorption measurements is, in fact, equal to the sum of the two equilibrium constants K// and Kanti//. If we suppose than these two constants are approximately equal, it leads to the conclusion that the Kanti//Pyr6G/Kanti//Rh6G ratio is equal to 2 instead of about 4.

IV.c. Design of Efficient Laser Dyes. From the previous discussion, it appears that supplementary hydrophilic groups on the Rhodamine chromophore are needed to obtain efficient laser dyes in aqueous solution. From this point of view, SO_3^- groups are particularly interesting because they also allow a substantial increase of the repulsive dye−dye interaction. Nevertheless, the position of these SO_3^- groups on the Rhodamine skeleton plays a non-negligible role.

Sulforhodamine dyes such as sulforhodamine 6 G still exhibits an appreciable dimerization constant ($K \sim 4000\ M^{-1}$ according to Drexhage[17]). On the contrary, the chemical group $N(CH_2)_nSO_3^-$ is very efficient. For example, the dimerization constant of the dye JA 7 [21] is about 200 M^{-1}. In our laboratory, we have synthesized the Rhodamine shown in Figure 14.

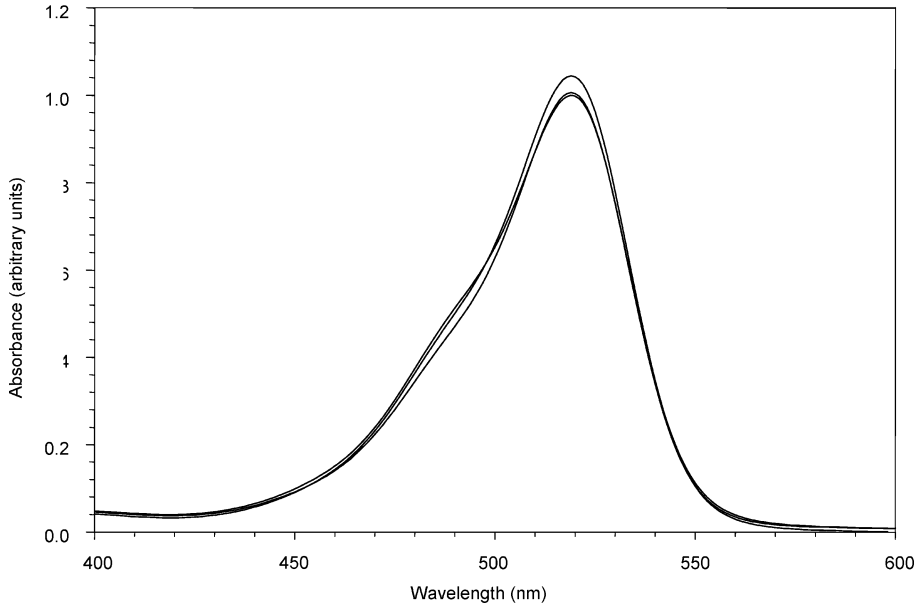

Figure 15. Normalized absorption spectra of the new synthesized dye for three dilutions (4×10^{-7}, 2×10^{-4}, and 5×10^{-4} M).

The normalized absorption spectra shown in Figure 15 for three dilutions in water (4×10^{-7}, 2×10^{-4}, and $5. 10^{-4}$ M) are identical. The blue-shifted peak, which characterizes the formation of a dimer, is missing. A rough estimate of the dimerization constant leads to a value smaller than 1.0 M^{-1}. In the concentration range corresponding to the current use of these dyes, no dimer appears.

V. Conclusions

The dimerization process of some charged xanthene derivatives in water solution has been evidenced by both T-ROESY experiments on one hand and by molecular dynamics simulations on the other hand. The experimental and theoretical results are in very good agreement. This study proves the ability of molecular dynamics simulations to accurately describe an apparently surprising result, the dimerization of charged species. The van der Waals dye−dye interaction and the interaction of the two dye molecules with their surroundings energetically favors the dimerization process. Moreover, no correlation between the dye−dye interaction and the dimerization equilibrium constant can be evidenced. Nevertheless, the concept of effective hydrophobic forces is very useful for the design of xanthene derivatives exhibiting no appreciable dimerization in water. From this point of view, the chemical group $N(CH_2)_nSO_3^-$ is particularly efficient, and we have synthesized such molecules with a dimerization equilibrium constant smaller than the standard corresponding values by at least 3 orders of magnitude. Finally, NMR results and dynamic molecular simulations clearly show that, in the Pyronine case, two dimers, parallel and antiparallel, coexist, separated by a noticeable free energy barrier and exhibiting very similar equilibrium constant. In such cases, the use of the standard photometric method, which cannot distinguish between these two species, leads to the determination of an effective equilibrium constant equal to the sum of the corresponding value for each dimer.

References and Notes

(1) Selwyn, J. E.; Steinfeld, J. I. *J. Phys. Chem.* **1972**, *76*, 762.
(2) Wong, M. M.; Schelly, Z. A. *J. Phys. Chem.* **1974**, *78*, 1891.
(3) Toptygin, D.; Packard, B. Z.; Brand, L. *Chem. Phys. Lett.* **1997**, *277*, 430.
(4) Ilich, P.; Mishra, P. K.; Macura, S.; Burghardt, T. P. *Spectrochim. Acta A* **1996**, *52*, 1323.
(5) Ajtai, K.; Burghardt, T. P. *Biochemistry* **1995**, *34*, 15943.
(6) Penzkofer, A.; Leupacher, W. *J. Lumin.* **1987**, *37*, 61.
(7) Gerschel, A. *Liaisons Intermoleculaires*; InterEditions/CNRS Ed: Paris, France, 1995.
(8) Troxler, L.; Harrowfield, J. M.; Wipff, G. *J. Phys. Chem. A* **1998**, *102*, 6821.
(9) Case, D. A.; Pearlman, D. A.; Caldwell, H. W.; Cheatham, T. E., III.; Ross, W. S.; Simmerling, C.; Darden, T.; Merz, K. M.; Stanton, R. V.; Cheng, A.; Vincent, J. J.; Crowley, M.; Ferguson, D. M.; Radmer, R.; Seibel, G. L.; Singh, U. C.; Weiner, P.; Kollman, P. A. *AMBER5*; University of California, 1997.
(10) Fischer, M.; Georges, J.; *Spectrochim. Acta Part A* **1997**, *53*, 1419.
(11) Kasha, M.; Rawls, H. R.; Ashraf El-Bayoumi, M. *Pure Appl. Chem.* **1965**, *11*, 371.
(12) Millié, P.; Langlet, J.; Berges, J.; Caillet, J.; Demaret, J.-P. *J. Phys. Chem B* **1999**, *103*, 10883.
(13) Frisch, M. J.; Trucks, G. W.; Schlegel, H. B.; Scuseria, G. E.; Robb, M. A.; Cheeseman, J. R.; Zakrzewski, V. G.; Montgomery, J. A., Jr.; Stratmann, R. E.; Burant, J. C.; Dapprich, S.; Millam, J. M.; Daniels, A. D.; Kudin, K. N.; Strain, M. C.; Farkas, O.; Tomasi, J.; Barone, V.; Cossi, M.; Cammi, R.; Mennucci, B.; Pomelli, C.; Adamo, C.; Clifford, S.; Ochterski, J.; Petersson, G. A.; Ayala, P. Y.; Cui, Q.; Morokuma, K.; Malick, D. K.; Rabuck, A. D.; Raghavachari, K.; Foresman, J. B.; Cioslowski, J.; Ortiz, J. V.; Stefanov, B. B.; Liu, G.; Liashenko, A.; Piskorz, P.; Komaromi, I.; Gomperts, R.; Martin, R. L.; Fox, D. J.; Keith, T.; Al-Laham, M. A.; Peng, C. Y.; Nanayakkara, A.; Gonzalez, C.; Challacombe, M.; Gill, P. M. W.; Johnson, B. G.; Chen, W.; Wong, M. W.; Andres, J. L.; Head-Gordon, M.; Replogle, E. S.; Pople, J. A. *Gaussian 98*, revision A.11.3; Gaussian, Inc.: Pittsburgh, PA, 1998.
(14) Jorgensen, W. L.; Chandrasekhar, J.; Madura, J. D. *J. Chem. Phys.* **1983**, *79*, 926.
(15) Lu, Y.; Penzkofer, A. *Chem. Phys.* **1986**, *107*, 175.
(16) Bojarski, C.; Obermueller, G. *Acta Phys. Pol.* **1976**, *A50*, 389.
(17) Sens, B.; Drexhage, K. H. Unpublished results.
(18) Lopez Arbeloa, F.; Llona Gonzalez, I.; Ruiz Ojeda, P.; Lopez Arbeloa, I. *J. Chem. Soc., Faraday Trans. 2* **1982**, *78*, 989.
(19) Lopez Arbeloa, F.; Ruiz Ojeda, P.; Lopez Arbeloa, I. *J. Chem. Soc., Faraday Trans. 2* **1988**, *84*, 1903.
(20) Scala-Valero, C. *Thesis Synthese et caracterisation de nouveaux colorants laser*; University of Orleans: Orleans, France, 1997.
(21) Arden-Jacob, J. *Thesis Neue langwellige Xanthen-Farbstoffe für Fluoreszensonden and Farbstofflaser*; Universität-Gesamthochschule Siegen, 1992.
(22) Pean, C.; Creminon, C.; Wijkhuisen, A; Perly, B.; Djedaïni-Pilard, F. *J. Chim. Phys.* **1999**, *96*, 1486.